

Evidence for the van Hove scenario in high-temperature superconductivity from quasiparticle-lifetime broadening

P. C. Pattnaik, C. L. Kane, D. M. Newns, and C. C. Tsuei

IBM Research Division, Thomas J. Watson Research Center, P.O. Box 218, Yorktown Heights, New York 10598

(Received 26 September 1990; revised manuscript received 19 July 1991)

Calculations of the quasiparticle-lifetime broadening $1/\tau$, both for idealized and realistic models of the band structure, show a large lifetime broadening from electron-electron scattering, with the characteristic linear dependence on energy from the Fermi energy seen in high-temperature superconductors, provided that the Fermi level lies near the van Hove singularity in the quasi-two-dimensional band structure. The effect comes from intra-van Hove-singularity scattering *without* the intervention of nesting.

High-temperature superconductors are remarkable not only for their high transition temperatures, but also for numerous normal-state properties differing qualitatively from a conventional metal. The largest group of such properties originates in the anomalous behavior of the quasiparticle lifetime τ . Considered as a function of energy ϵ from the Fermi level, τ has the behavior $1/\tau(\epsilon) \propto \epsilon$. This has been directly observed in angle-resolved photoemission¹ and by infrared-reflectivity measurements² up to $\epsilon \sim 0.3$ eV, while the same result can be inferred from the linearity of the resistivity as a function of temperature and from other frequency and temperature dependences.³ The anomalous lifetime seems incompatible with conventional phonon scattering, for which $1/\tau(\epsilon)$ should tail off above the Debye temperature, say, above 0.04 eV, while electron-electron scattering on a cylindrical Fermi surface leads to $\epsilon^2 \ln \epsilon$ behavior,⁴ which is much too weak at low energies. In this paper we shall demonstrate that the anomalous lifetime broadening follows from the presence of the van Hove singularity (vHS), previously introduced in discussions of the superconducting properties of the oxide superconductors^{6,7} and of the vHS alone.

The assumption behind the van Hove scenario⁵⁻⁷ is that the Fermi level in high-temperature superconductors lies close to the energy E_{vHS} of the van Hove singularity in their quasi-two-dimensional (quasi-2D) density of states. Direct support for this assumption comes from slave-boson renormalized band-structure studies of the 2:1:4 and 2:2:1:2 materials,⁷ in which E_F coincides with E_{vHS} at 13% and 34% doping, respectively, and in which it is found that the Fermi level is pegged near the van Hove singularity for doping variations of $\pm 25\%$ around these values. It is important to recognize that the occurrence of $E_F = E_{\text{vHS}}$, which we term the van Hove condition, does not also imply a nesting condition, although this coincidence of the van Hove and nesting conditions does occur in one special case, the half-filled Hubbard model on a square lattice with nearest-neighbor hopping.⁸ The nesting condition is undesirable because it generates spin-density-wave (SDW) and charge-density-wave (CDW) fluctuations inimical to superconductivity, but fortunately in reality⁷ the van Hove condition occurs far from the half-filling point, where there is limited nesting.

It is well known that^{5,6} the effect of E_F lying close to

the vHS within BCS theory is to enhance T_c , which has a maximum at the van Hove condition.^{5,6} Moreover, it is also found that the isotope shift is anomalous, becoming a strong function of the location of the Fermi level, with a minimum at the van Hove condition;⁵ this anomalous behavior of the isotope shift is consistent with recent observations.⁹ It is seen that the maximum- T_c material in a given variable-composition oxide superconductor system may be interpreted, within the van Hove scenario, as the material in which the van Hove condition is satisfied.

The lifetime broadening of a quasiparticle at a point \mathbf{k} on the Fermi surface is calculated from the expression⁴

$$1/\tau(\mathbf{k}, \omega) = 2 \text{Im} \Sigma(\mathbf{k}, \omega), \quad (1)$$

where the self-energy Σ is determined from the Feynman diagram illustrated in Fig. 2. The electron-electron interaction W appearing in the diagram is assumed to be an instantaneous δ -function interaction; i.e., $W(\mathbf{q}, \omega)$ is independent of \mathbf{q} and ω .

An analytic expression for the lifetime broadening of low-energy quasiparticles has been given,¹⁰ for the case of the idealized model of a vHS at half filling

$$\epsilon_{\mathbf{k}} = k_x k_y, \quad (2)$$

defined within the square Brillouin zone (BZ) with corners at $\mathbf{k} = (\pm k_c, \pm k_c)$. This model is non-nested even when considered in the extended-zone scheme. For the dispersion (2), the analytic result for the on-shell relaxation time is

$$\begin{aligned} 1/\tau(\epsilon_{\mathbf{k}}) &= 2 \text{Im} \Sigma(\mathbf{k}, \epsilon_{\mathbf{k}}) \\ &= 2\pi \left[\frac{W}{D} \right]^2 \epsilon_{\mathbf{k}} [1 - \eta(k_x/k_c) - \eta(k_y/k_c)], \end{aligned} \quad (3)$$

where $D = k_c^2$ and

$$\eta(x) = \frac{1}{4} [(1/x) \ln(1-x^2) + \ln|(1+x)/(1-x)|].$$

In Fig. 1 we plot (3) and compare it with a direct numerical evaluation of the on-shell relaxation times $1/\tau(\epsilon_{\mathbf{k}})$ from (1) and (2). The behavior of $1/\tau$ at small \mathbf{k} shows the universal scaling with $\epsilon_{\mathbf{k}}$ from (3), whereas at larger \mathbf{k} the curves bend over in a manner no longer depending universally on $\epsilon_{\mathbf{k}}$ and, also, expected from (3). The analytic expression (3) uses a small- \mathbf{k} approximation to treat

the polarizability in the Feynman diagram in Fig. 2; hence its large- k behavior differs quantitatively from the numerical data, although Eq. (3) gives an excellent qualitative account of the behavior over the whole range. The nonuniversal behavior at large k seen in Fig. 1 does not seem to be general and depends on how the large- k cutoff is introduced into the model.

In the inset in Fig. 1, we illustrate the $1/\tau$ defined off shell for \mathbf{k} on the Fermi surface (FS) i.e., $1/\tau(\omega) = 2 \text{Im}\Sigma(\mathbf{k}_F, \omega)$. This is done for a model with hyperbolic energy surfaces, and with ε_F at the vHS, the same model with ε_F shifted away from the vHS and a model with a cylindrical Fermi surface lacking any vHS. It is seen from the inset how the linear scaling $1/\tau(\omega) \propto \omega$ goes over to the $\omega^2 \ln \omega$ behavior characteristic of a cylindrical FS.⁴ The hyperbolic model in the inset has a different cutoff from (2) (see figure caption for details), which does not lead to the saturating tendency at large ω .

It should be stressed that in the model of Eq. (2) there is only one vHS; hence there can be no nesting or inter-vHS scattering. The anomalous $1/\tau$ comes purely from the extra phase space available for scattering parallel to the asymptotes when the van Hove condition is satisfied. Hence we can distinguish the origin of the anomalous $1/\tau$ calculated in this paper from the nested Fermi-liquid scattering of Virostek and Ruvalds¹¹ and from the inter-van Hove-singularity scattering effect calculated by Lee and Read,⁸ and applied by Markiewicz.⁸ As men-

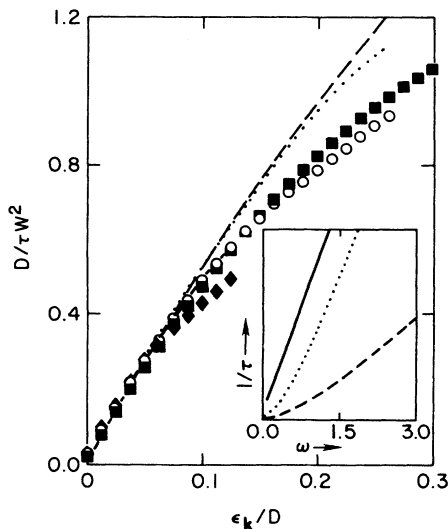


FIG. 1. Plot of the on-shell $1/\tau(\varepsilon_k) = 2 \text{Im}\Sigma(\mathbf{k}, \varepsilon_k)$ for the hyperbolic model of Eq. (2); diamonds, $k_y = 0.16k_c$; circles, $k_y = 0.32k_c$; squares $k_y = 0.48k_c$; $D = k_c^2$. Curves, Eq. (3); k_y values as above for solid, dotted, and dashed curves, respectively. Inset, plot of $1/\tau(\omega) = 2 \text{Im}\Sigma(\mathbf{k}_F, \omega)$ from (1) vs energy ω from Fermi energy, for hyperbolic ($\varepsilon_k = kx^2/2 - ky^2/2$) and free-electron ($\varepsilon_k = kx^2/2 + ky^2/2$) dispersion in $2\pi \times 2\pi$ Brillouin zone, with \mathbf{k} on the Fermi surface. Solid curve, hyperbolic, van Hove condition $E_F = 0$, with half of the zone occupied by FS, $\mathbf{k} = (0.234, 0.234)\pi$. Dotted curve, hyperbolic, $E_F = 0.405, 0.4$ zone occupied, $\mathbf{k} = (0.370, 0.243)\pi$. Dashed curve, free electron, $E_F = \pi^2/2$, with 0.25 of zone occupied, $\mathbf{k} = (\sqrt{\pi/2}, \sqrt{\pi/2})$. (Results are found to be insensitive to the precise location of \mathbf{k} on the FS.)

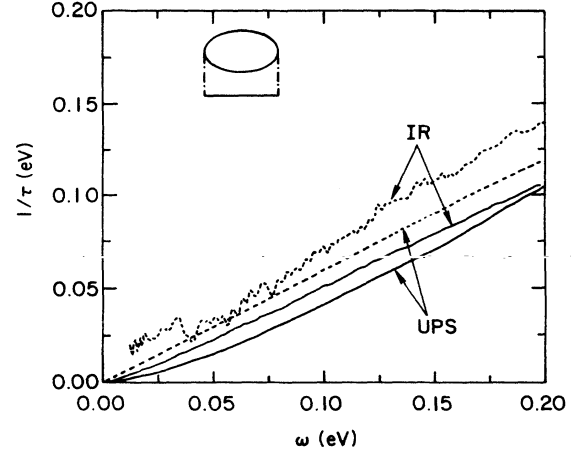


FIG. 2. Inset, Feynman diagram for the self-energy $\Sigma(\mathbf{k}, \omega)$. Solid curves describe the theoretical quasiparticle-lifetime broadening, $1/\tau(\omega)$, at doping $x = 0.3$ (which differs from the van Hove condition by several percent). Dashed curves are experimental results from infrared (Ref. 2) and photoemission (Ref. 1). In the ir calculation, $1/\tau(\omega)$ is calculated from (1), with \mathbf{k} averaged over the Fermi surface. In the photoemission calculation, \mathbf{k} in (1) is located along the ΓX direction such that $\omega = \varepsilon_{\mathbf{k}}$; the curve can be parametrized by $\tau^{-1}(\omega) = 0.36\omega + 0.88\omega^2$, (in units of eV).

tioned above, this is a key distinction because the nesting intrinsic to these earlier models of anomalous scattering also has the undesirable feature of introducing SDW and CDW fluctuations which are inimical to s -wave superconductivity. In contrast, the present model, which relies entirely on intra-van Hove-singularity scattering, enhances superconductivity without introducing undesirable SDW or CDW fluctuations.

When there are multiple van Hove singularities, inter-van Hove-singularity scattering can occur, but such inter-vHS scattering only leads to the anomalous phase space considered by Lee and Read,⁸ and, hence, to the linear scaling for $1/\tau$ with energy when the asymptotes to the hyperbolic energy surfaces are *orthogonal*. We give a mathematical demonstration of this in the Appendix.

In addition to the foregoing model systems, we also implement the calculation for the realistic model of the CuO_2 plane considered in Ref. 7. The model, based on the 2:2:1:2 material, includes the Cu $3d$ and the oxygen $2p_x$ and $2p_y$ orbitals, with matrix elements derived from the NRL parametrization of the 2:2:1:2 band structure.¹² The Cu $3d$ -orbital energy was adjusted to allow for an accurate fit to the angle-resolved photoemission data by the slave-boson technique.⁷ The interaction W , expected to be of order E_F , was taken to be 1.3 times the electron Fermi energy of 0.48 eV. This model, which has two degenerate van Hove singularities at $(\pi/a, 0)$ and $(0, \pi/a)$, is also non-nested because the asymptotes of the hyperbolas describing the energy surfaces close to the vHS's are extremely nonorthogonal; only in the orthogonal case does nesting occur.

First, we consider the lifetime for a wave vector \mathbf{k} lying along a particular direction, Γ to X , in the Brillouin zone of our model. This is illustrated in Fig. 2 and compared

with the results of angle-resolved photoemission.¹ The fit is seen to be fair, but the theoretical plot is significantly curved relative to the experimentalists' linear fit to the angle-resolved photoemission-spectroscopy (ARPS) data. It is possible that this curvature could lie within experimental uncertainties, since more recent analysis of these ARPS data showed that it is also consistent with a parabolic fit.¹³ We also calculate the lifetime averaged over the Fermi surface and compare this with infrared data² in Fig. 2. The agreement is significantly better than in the photoemission case.

We arrive at the remarkable conclusion that the behavior of the lifetime due to electron-electron scattering is transformed by the presence of the vHS. $1/\tau(\epsilon)$ becomes a linear function of ϵ and has the right magnitude compared with the experimental data. This provides strong support for the van Hove scenario, whereby the requirement of maximum T_c places the Fermi level close to the van Hove singularity, giving rise to a series of anomalous properties. In our case this includes the linear resistivity, which follows from the linearity in ϵ of the Fermi-surface-averaged lifetime; although a linear resistivity is also found in electron-phonon scattering in the presence of the vHS,¹⁴ this mechanism cannot, as discussed above, explain the energy dependence of $1/\tau$.

Further evidence linking the linear behavior of $1/\tau$ with the vHS comes from the dependence of resistivity-temperature curves on doping. It is found that $\rho(T)$ ceases to be linear in low- T_c materials or when variations in doping away from the T_c maximum are considered.¹⁵ Our interpretation is that the T_c maximum is itself brought about by the closeness of the Fermi level to the vHS; hence the linear resistivity is expected to occur in the neighborhood of the T_c maximum.

The perturbational approximation that we are using is in principle only valid in weak coupling, and for the strong-coupling situation the $1/N$ expansion provides a better basis for the calculation. To leading order in $1/N$, the same diagram as in Fig. 2 may be used if the interaction W is reinterpreted; it is related to the real part of the slave-boson response function. Calculations in the strong-coupling region remain to be carried out.

Many cuprate systems are disordered as a result of concentrations of order 15% of dopant. Impurity scattering, if strong enough, might destroy the vHS effects described in this Brief Report. However, the dopant is invariably located¹⁶ outside the CuO_2 plane in cuprate superconductors, and this type of doping can be thought of as a form of the very successful modulation doping technique used in semiconductor superlattices which allows doping to be implemented with minimal effect on the elastic mean free path. Effects which tend to reduce Coulomb scattering of the carriers in the plane by the dopant are (a) screening by the carrier electron gas, (b) screening by the rest of the dielectric medium, and (c) the z factor in a strongly correlated electron gas. If screening reduces the scattering potential by a factor of, say, at least 4, i.e., the Born cross section by at least 16, and the z factor takes the value of approximately $7\frac{1}{3}$, then a reduction in the scattering cross section by two orders of magnitude over the bare Coulomb cross section is to

be expected. This should be sufficient to explain the low residual resistivities observed and to permit the vHS effect to be undiminished by impurity scattering.

The anomalously large electronic quasiparticle-lifetime broadening may provide an explanation for the lack of correlation between the low λ and the large energy-gap-to- T_c ratio observed for many high- T_c cuprate superconductors.¹⁵ It could provide also an alternative to strong inelastic electron-phonon scattering¹⁷ as a mechanism for suppressing the coherence peak in ir conductivity and spin-lattice relaxation-time measurements.

The present calculation shows that the major anomalous property of the normal state of high-temperature superconductors, the quasiparticle lifetime, can be explained by extending the conventional lifetime-broadening calculation so as to take the van Hove singularity into account. At the thermodynamic level, the vHS also provides an explanation⁷ for the high density of states at the Fermi level, which would otherwise seem incompatible with the relatively light mass deduced from the angle-resolved photoemission data.¹ Calculations of other key properties are under way.

We are grateful to John C. C. Chi and H. R. Krishnamurthy for valuable discussions and to R. T. Collins and Z. Schlesinger for use of their data.

APPENDIX

In this appendix we demonstrate that the mechanism for linear scaling of lifetime broadening with energy, coming from inter-van Hove-singularity scattering, found by Lee and Read (LR)⁸ is a special result associated with the case where the vHS has orthogonal asymptotes. The LR mechanism is thus unlikely to be important except for the unique case they considered of the half-filled nearest-neighbor coupling Hubbard model on a square lattice. In general, inter-van Hove-singularity scattering does not lead to a linear scaling of the lifetime broadening, and such scaling comes in general from the scattering around a single vHS considered in this paper. Consider a square BZ with two vHS's located at $\mathbf{k}=(0,0)$ and at $\mathbf{k}=(-\pi,\pi)=\mathbf{Q}$: Let

$$\begin{aligned}\epsilon_{\mathbf{k}1} &= -\alpha^2 k_x^2 + \beta^2 k_y^2 \quad (\beta > \alpha), \\ \epsilon_{\mathbf{k}2} &= \beta^2 (k_x + \pi)^2 - \alpha^2 (k_y - \pi)^2.\end{aligned}$$

Lee and Read find [their Eq. (4)] that for a wave vector $\mathbf{q}=\mathbf{Q}$ the imaginary part of the susceptibility

$$\text{Im}\chi(\mathbf{Q},\omega) \sim \ln\omega.$$

Now

$$\begin{aligned}\text{Im}\chi(\mathbf{Q},\omega) &= \sum_{\mathbf{k}} (f_{\mathbf{k}+\mathbf{Q}} - f_{\mathbf{k}}) \delta(\epsilon_{\mathbf{k}2+\mathbf{Q}} - \epsilon_{\mathbf{k}1} - \omega) \\ &= \sum_{\mathbf{k}} (f_{\mathbf{k}+\mathbf{Q}} - f_{\mathbf{k}}) \delta((\alpha^2 + \beta^2)(k_x^2 - k_y^2) - \omega) \\ &= \frac{1}{\alpha^2 + \beta^2} \sum_{\mathbf{k}} (f_{\mathbf{k}+\mathbf{Q}} - f_{\mathbf{k}}) \\ &\quad \times \delta(k_x^2 - k_y^2 - \omega/(\alpha^2 + \beta^2)).\end{aligned}$$

Case a: $\alpha \neq \beta$

One branch of the hyperbola,

$$k_x^2 - k_y^2 = \omega / (\alpha^2 + \beta^2),$$

is shown in Fig. 3(a) as L . L intercepts the occupied one Fermi surface at

$$k_y^* = \pm \alpha [\omega / (\beta^4 - \alpha^4)]^{1/2} \sim \sqrt{\omega},$$

$$k_x^* = \beta [\omega / (\beta^4 - \alpha^4)]^{1/2}.$$

Replacing $\Sigma_{\mathbf{k}}$ by $\int dk_x \int dk_y$,

$$\text{Im}\chi(\mathbf{Q}, \omega) = 1 / (\alpha^2 + \beta^2)$$

$$\times \int dk_x \int dk_y \delta([k_x - (k_y^2 + A^2)^{1/2}] \times [k_x + (k_y^2 + A^2)^{1/2}]),$$

where

$$A^2 = \frac{\omega}{\alpha^2 + \beta^2}.$$

Evaluating the contribution of the first square root as an example,

$$\begin{aligned} \text{Im}\chi(\mathbf{Q}, \omega) &= \frac{1}{\alpha^2 + \beta^2} \int_0^{k_y^*} dk_y \frac{1}{(k_y^2 + A^2)^{1/2}} \\ &= \frac{1}{\alpha^2 + \beta^2} \ln \left\{ \frac{k_y^*}{A} + \left[1 + \left(\frac{k_y^*}{A} \right)^2 \right]^{1/2} \right\}. \end{aligned}$$

Since $k_y^*/A = \text{const}$ ($\omega \rightarrow 0$),

$$\text{Im}\chi(\mathbf{Q}, \omega) = \text{const} \quad (\text{with } \omega \text{ small}).$$

This shows that the imaginary part of the susceptibility tends to a constant at small ω , lacking the logarithmic divergence crucial to the Lee-Read argument.

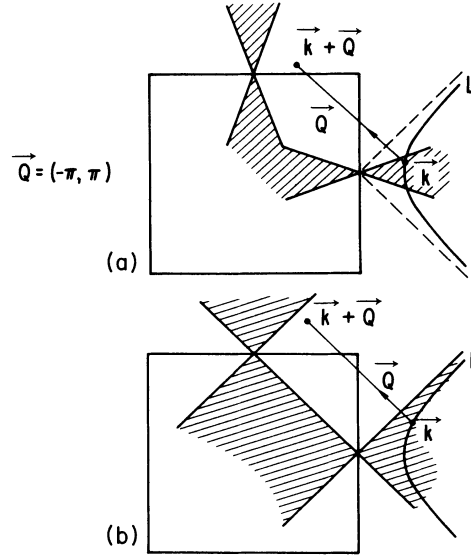


FIG. 3. Sketch for calculation of inter-van Hove-singularity contribution to the susceptibility (see text).

Case b: $\alpha = \beta$

The difference here [see Fig. 3(b)] is that the allowed region of \mathbf{k} runs over the whole van Hove singularity region up to the cutoff k_c . Now the integral gives

$$\text{Im}\chi(\mathbf{Q}, \omega) \simeq \frac{1}{2(\alpha^2 + \beta^2)} \ln \left[\frac{4k_c^2(\alpha^2 + \beta^2)}{\omega} \right].$$

Here we retrieve the logarithmically singular susceptibility found by Lee and Read.

- ¹C. G. Olson, R. Liu, D. W. Lynch, R. S. List, A. J. Arko, B. W. Veal, Y. C. Chang, P. Z. Jiang, and A. B. Paulikas (unpublished); J. C. Campuzano, G. Zennings, M. Faig, L. Beau-laigue, B. W. Veal, J. Z. Liu, A. P. Paulikas, K. Vandervoort, H. Claus, R. S. List, A. J. Arko, and R. J. Bartlett, Phys. Rev. Lett. **64**, 2308 (1990).
- ²Z. Schlesinger, R. T. Collins, F. Holtzberg, C. Field, S. H. Blanton, U. Welp, G. W. Crabtree, Y. Fang, and J. Z. Liu, Phys. Rev. Lett. **65**, 801 (1990).
- ³C. M. Varma, P. B. Littlewood, S. Schmitt-Rink, E. Abrahams, and A. E. Ruckenstein, Phys. Rev. Lett. **63**, 1996 (1989); **64**, 497 (E) (1990).
- ⁴C. Hodges, H. Smith, and J. W. Wilkins, Phys. Rev. B **4**, 302 (1971).
- ⁵C. C. Tsuei, D. M. Newns, C. C. Chi, and P. C. Pattnaik, Phys. Rev. Lett. **65**, 2724 (1990).
- ⁶J. Friedel, J. Phys. (Paris) **48**, 1787 (1987); **49**, 1435 (1988); J. Labbe and J. Bok, Europhys. Lett. **3**, 1225 (1987); R. S. Markiewicz and B. J. Giessen, Physica C **160**, 497, (1989); Phys. Scr. **37**, 940 (1988); R. S. Markiewicz, J. Phys. Condens. Matter **1**, 8911 (1989); **1**, 8931 (1989); J. E. Dzyaloshinskii, Pis'ma Zh. Eksp. Teor. Fiz. **46**, 97 (1987) [JETP Lett. **46**, 118 (1987)]; Zh. Eksp. Teor. Fiz. **93**, 1487 (1989) [Sov. Phys.—JETP **66**, 848 (1989)], and references therein.
- ⁷D. M. Newns, P. C. Pattnaik, and C. C. Tsuei, Phys. Rev. B **43**, 3075 (1991); D. M. Newns, P. C. Pattnaik, M. Rasolt, and D. A. Papaconstantopoulos, *ibid.* **38**, 7033 (1988).

- ⁸P. A. Lee and N. Read, Phys. Rev. Lett. **58**, 2691 (1987), R. S. Markiewicz, *ibid.* **62**, 603 (1989).
- ⁹M. K. Crawford, M. N. Kunchur, W. E. Farneth, E. M. McCarron, and S. J. Poon, Phys. Rev. B **41**, 282 (1990); J. P. Franck, J. Jung, M. A. K. Mohamed, S. Gygax, and I. G. Sproule, Physica B **169**, 697 (1991); H. J. Bornemann and D. E. Morris (unpublished).
- ¹⁰C. Kane, D. M. Newns, P. C. Pattnaik, C. C. Tsuei, and C. C. Chi, in *Electronic Structure and Mechanisms for High Temperature Superconductivity*, edited by J. Ashkenazi and G. Vessoli (Plenum, New York, in press).
- ¹¹A. Virostek and J. Ruvalds, Phys. Rev. B **42**, 4064 (1990); J. Ruvalds and A. Virostek, *ibid.* **43**, 1996 (1990); J. Ruvalds, Phys. Rev. Lett. **67**, 1657 (1991).
- ¹²M. J. DeWeert, D. A. Papaconstantopoulos, and W. E. Pickett, Phys. Rev. B **39**, 4235 (1989); D. A. Papaconstantopoulos (private communication).
- ¹³L. Z. Liu, R. O. Anderson and J. W. Allen (unpublished).
- ¹⁴Qimiao Si and K. Levin, in *Electronic Structure and Mechanisms for High Temperature Superconductivity* (Ref. 10).
- ¹⁵C. C. Tsuei, A. Gupta, and G. Koren, Physica C **161**, 415 (1989); C. C. Tsuei, Physica A **168**, 238 (1990).
- ¹⁶The exception, Zn doping, goes into the planes, but thereby causes strong scattering, as evidenced by a large increase in the residual resistivity and a reduction in T_c .
- ¹⁷P. B. Allen and D. Rainer, Nature **349**, 396 (1991); J. P. Carbotte and E. J. Nicol, Physica C **185-189**, 162 (1991).